Observation of Forward Shocks and Stagnated Ejecta Driven by High-Energy-Density Plasma Flow

R. P. Drake,[1] S. G. Glendinning,[2] Kent Estabrook,[2] B. A. Remington,[2] Richard McCray,[3] R. J. Wallace,[2] L. J. Suter,[2] T. B. Smith,[1] J. J. Carroll III,[1] R. A. London,[2] and E. Liang[4]

[1]*University of Michigan, Ann Arbor, Michigan 48109*

[2]*Lawrence Livermore National Laboratory, Livermore, California 94551*

[3]*University of Colorado, Boulder, Colorado 80309*

[4]*Rice University, Houston, Texas 77251*

(Received 9 September 1997; revised manuscript received 8 June 1998)

Laboratory studies of hydrodynamic effects driven by a flowing, expanding plasma of high-energy density and high Mach number are reported. The flowing plasma is the ejecta from matter accelerated and heated by an ablative shock. X-ray backlighting diagnoses the structure produced when this plasma impacts low-density foam. We observe the forward shock driven into the foam and the stagnated ejecta which drives a reverse shock into the flow. [S0031-9007(98)07075-6]

PACS numbers: 52.50.Lp, 47.40.Nm, 52.35.Tc

The hydrodynamics of high-energy-density plasma has been an active area of study in recent years, motivated by applications from inertial fusion [1] to equation of state (EOS) studies [2] to supernovae [3]. A major focus in these studies has been the hydrodynamic effects driven by the ablation of matter, resulting from irradiation by lasers [4] or by x rays [5–14]. We present here work on a complementary problem—the hydrodynamic effects driven by the impact of energetic, flowing, expanding plasma upon matter. Such situations abound in the natural universe and there have been many theoretical studies of them, for example, in the heliosphere [15] and in supernova remnants [16–19]. We report here the first laboratory study, to our knowledge, of hydrodynamic structures driven by a plasma flow at $\sim$100 km/s.

In ablation-driven hydrodynamics, ablation pressure drives a shock forward into uncompressed material, while the ablated material expands and rarefies away from the surface. In flow-driven hydrodynamics, stagnation pressure drives a shock forward into uncompressed material, as long as the incoming flow has sufficient velocity. The flowing plasma is slowed to the velocity of the contact surface between the materials, and in this sense can be said to stagnate. If the pressure in the incoming plasma is low enough, relative to its kinetic energy, then a reverse shock develops in the flowing plasma. It moves more slowly, in the laboratory frame, than the contact surface. In the present paper we report the first laboratory observation, to our knowledge, of such structures driven by a high-velocity plasma flow.

Plans for the experiments reported here were discussed in three paragraphs in Ref. [3]. That paper showed data from the single, demonstration laser shot which had been performed at that time and discussed the feasibility and potential applications of experiments of this type. The present paper reports the results of the first two sequences of experiments devoted to quantitative measurements of the behavior of such a system and reports the results of comparisons with simulations.

The experiment used the Nova laser facility [20]. The design involves a "package" (see Fig. 1) which is attached to the bottom of a laser-heated, cylindrical gold cavity (a hohlraum). We used a previously developed method [21] to produce an ablation-driven, planar shock which becomes the source of our flowing plasma. For the data shown below, 18 ± 2 kJ of laser energy at 0.35 μm laser wavelength, in a 0.97 ± 0.02 ns FWHM, flat-topped pulse, heats the 3-mm-long by 1.6-mm-diam hohlraum to a radiation temperature of 215 ± 5 eV. Time in the following is referenced to the half maximum of the laser pulse on its rising edge. This is a well-characterized "Nova Scale 1.0" configuration [22,23].

The x-ray flux from the hohlraum ablates a $\sim$200 μm thick plastic plug. One sequence of experiments used $C_{50}H_{44}Br_6$ plugs; the second used $C_{50}H_{48}Br_2$. The Br

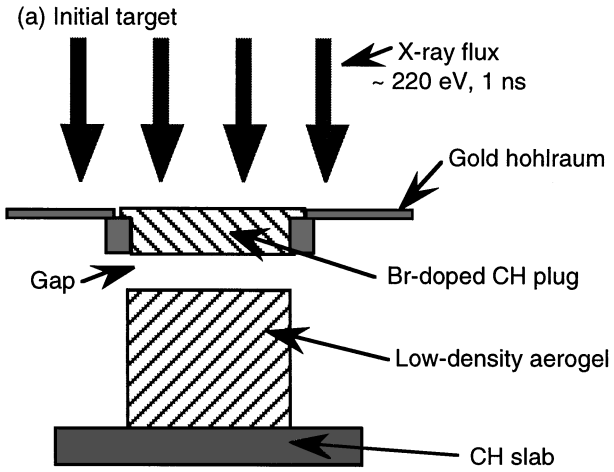

FIG. 1. The experimental package that is driven by a standard hohlraum x-ray source.

 0031-9007/98/81(10)/2068(4)$15.00

doping reduces the transmission of higher-energy x rays. The plug is mounted in a ~700-μm-diam hole in a gold washer attached to the hohlraum. The ablation of the plug by the x rays drives a strong shock through it. In the simulations discussed below, just prior to shock breakout, the postshock pressure and temperature were approximately 25 Mbar and 20 eV, respectively. We used a UV streak camera to measure the breakout of the shock. This occurred at 3.3 $\pm$ 0.3 ns from a 205 $\pm$ 1 μm thick plug of $C_{50}H_{44}Br_6$ (density $\rho_1 = 1.54$ g/cm^3) and at 2.9 $\pm$ 0.1 ns from a 205 $\pm$ 1 μm thick plug of $C_{50}H_{48}Br_2$ (density $\rho_2 = 1.22$ g/cm^3). The observed ratio of shock breakout times equals $\sqrt{\rho_1/\rho_2}$, as expected for constant ablation pressure (assuming similar EOS). Once the shock breaks out of the back of the plug, plasma ejecta are released. The released plasma ejecta expand, cool, and accelerate across a ~150 μm wide gap. This flowing, expanding matter is the plasma flow.

The plasma flow impacts and accelerates low-density SiO_2 aerogel foam, of initial density 40 $\pm$ 4 mg/cm^3, producing a strong forward shock. We chose the foam density to be large enough that radiation preheat by emission from the shocked matter would be small. The pressure of the stagnating ejecta produces a reverse shock in the plasma flow. We designed the experiment using both one- and two-dimensional (1D and 2D) radiation-hydrodynamic simulations with the Lagrangian code, LASNEX [24]. We modeled the system in planar geometry using a radiation temperature source at the inner boundary of the plug. We used average ion (XSN) opacities [25]. The results obtained using QEOS formulas [26] did not differ significantly from those obtained using EOS tables. The absolute spectrum of the hohlraum x rays corresponded to experimental irradiation conditions. For the $C_{50}H_{48}Br_2$ plug, the treatment of radiation transport was important. In this case, a multigroup diffusion model was not accurate. We used a discrete-ordinate [27] radiation transport model for the simulations discussed here. The 2D simulations helped determine geometric details such as the optimum ratio of plug diameter to foam diameter (unity).

The 1D and 2D simulations produced the same gross hydrodynamic behavior near the axis for the duration of the experiment, to within 200 ps over 10 ns. Practical 2D simulations, however, are not very well resolved. Since we are better able to resolve the axial flow with 1D simulations, we show in Fig. 2 axial profiles from such a run. The expanding ejecta flows in from the left, with decreasing density ρ, pressure p, ion temperature T_i, and a flow velocity u that increases linearly with distance. At the reverse shock, u abruptly drops and ρ, p, and T_i increase. There is a density minimum at the contact surface, and all quantities drop abruptly at the forward shock.

We diagnosed the spatial structure with x-ray backlighting, using methods described previously [13]. A planar slab of Fe (or Sc) was mounted behind the target, where it was irradiated by two of the Nova laser beams in succession. The resulting K-shell x rays (6.7 keV for Fe or 4.3 keV for Sc) were transmitted through the target, apertured by a 400-μm-wide slit, and detected by an intensified x-ray framing camera. The framing camera, described elsewhere [28], obtained gated images of the target for which the FWHM of the gain was 80 ps. We determined the spatial shape of the backlighter source, with nearly identical results, by direct measurement of the backlighter spot on a separate laser shot or by fitting the shape of the backlighter signal as seen through undisturbed parts of the target. We calibrated the optical depth by using the known transmission through undisturbed parts of the target.

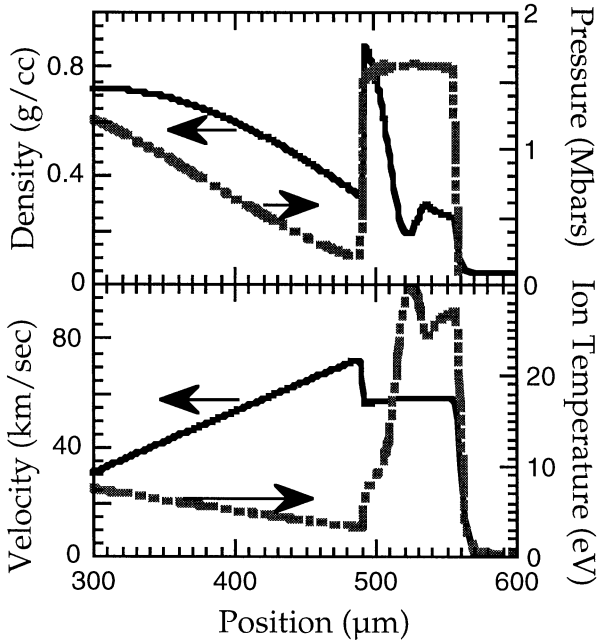

FIG. 2. Profiles at 8 ns calculated by a hydrodynamic simulation of the experiment, with the abscissa showing distance from the initial inner plug surface. The simulation used a $C_{50}H_{44}Br_6$ plug.

Figure 3 shows images of the optical depth obtained by this method, at 6.1 $\pm$ 0.1 ns and 9.1 $\pm$ 0.1 ns, and also shows the optical depth, averaged across the image, from experiments using a $C_{50}H_{48}Br_2$ plug. The forward shock and the peak of the stagnated ejecta are labeled. The shock fronts are spread beyond the nominal 10 μm resolution of the framing camera. We attribute the spreading both to parallax and to the alignment of the flat surfaces along which the measurements are made. We estimate the consequent width of a sharp, small step in optical depth to be ~30 μm. In the cases shown, the forward shock has propagated 150 μm (a), (b) and more than 450 μm (c), (d) through the foam. It is notable that the forward shock is well defined and is quite planar within the region defined by the 400 μm slit. The 2D expansion of the ejecta and the foam, which will eventually occur, is not yet large enough to affect these data. An independent measurement, without slits, made

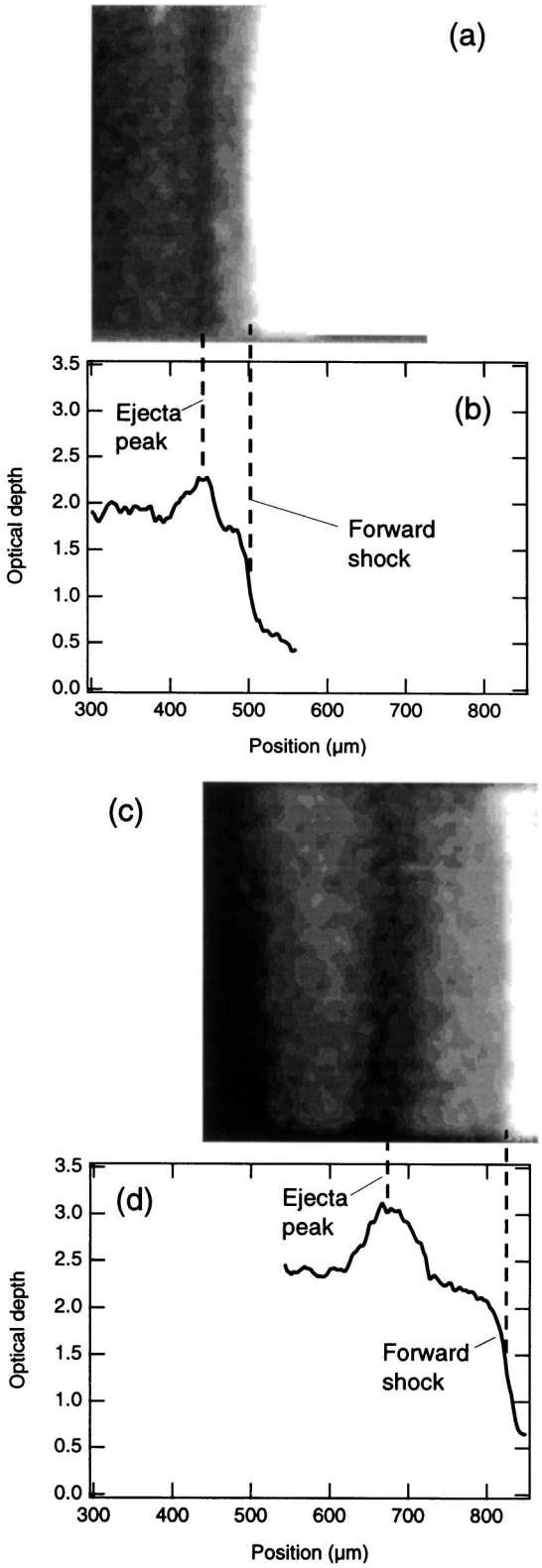

FIG. 3. Grayscale images (a), (c) and spatially averaged lineouts (b), (d) of the measured optical depth at 6 ns (a), (b) and 9 ns (c), (d).

along a perpendicular line of sight, showed the forward shock to be curved near the edges while remaining planar near its center.

Figure 4 shows data and simulation results for the two sequences of experiments. In both cases, the simulations reproduce the observed shock breakout time. In the case of the $C_{50}H_{44}Br_6$ plug [Fig. 4(a)], the simulation reproduces the observed velocities of the ejecta, the forward shock, and the ejecta peak to within the uncertainties. The forward shock in the simulation appears to be ahead of the observed shock, but the difference ($\sim 1/4$ ns) is marginal. Based on least-squares fits, the forward shock and ejecta peak velocities implied by the data of Fig. 4(a) are 68 ± 1 and 55 ± 1 km/s, respectively. The corresponding simulation curves give 67 and 51 km/s. If the level of preheat calculated by the simulations is correct, the upstream Mach number of the forward shock is ~ 30. In the case of the $C_{50}H_{48}Br_2$ plug [Fig. 4(b)], the simulation underestimates the velocity of the forward shock, the velocity of the ejecta peak, and the separation between them. The observed velocities of the forward shock and the ejecta peak, from least-squares fits, are 107 ± 3 and 77 ± 4 km/s, respectively. The corresponding simulation curves give 84 and 62 km/s. This difference between the data and the simulation results is discussed next.

The difference occurs late in time. Radiation effects are negligible then, as confirmed by simulations run with and without radiation transport after 3 ns. This is as expected, because we designed the system so that radiation from the hohlraum would be stopped by the brominated plastic, and so that the amount of preheat due to emission from the shocked $C_{50}H_{48}Br_2$ or the stagnated ejecta would be small. In other experiments using similar targets [2], the preheat was too small to cause changes in the foam density.

The observed separation between the ejecta peak and the forward shock implies an effective adiabatic index (γ) of the foam. Both the simulations and the observed separation of Fig. 4(a) correspond to $\gamma \sim 1.4$. The observed separation of Fig. 4(b) is much closer to that expected for $\gamma \sim \frac{5}{3}$. We have identified two possible explanations. First, the EOS of the foam might be incorrect. The experimental database for foams in this pressure regime is quite limited, and the theory is not trivial. Second, the electron preheat might not be negligible. Preheat could potentially increase γ by breaking chemical bonds and ionizing the foam. There is also some past evidence of unanticipated preheat [11] under similar conditions. Further exploration of these issues is, however, a subject of future research.

The flow-driven system demonstrated here has several potential applications. It can be used for the general study of hydrodynamics at high-energy density, for which it has the advantage that the hydrodynamics is decoupled from the details of the energy source. It can be used for hydrodynamic instability studies, as the stagnated ejecta near the contact surface are Rayleigh-Taylor unstable and as the forward shock wave can be sustained for a long period. It has application to astrophysics, as there are many astrophysical systems in which flow-driven hydrodynamics is essential. It can provide the first experimental tests of the computer models used for much interpretation of

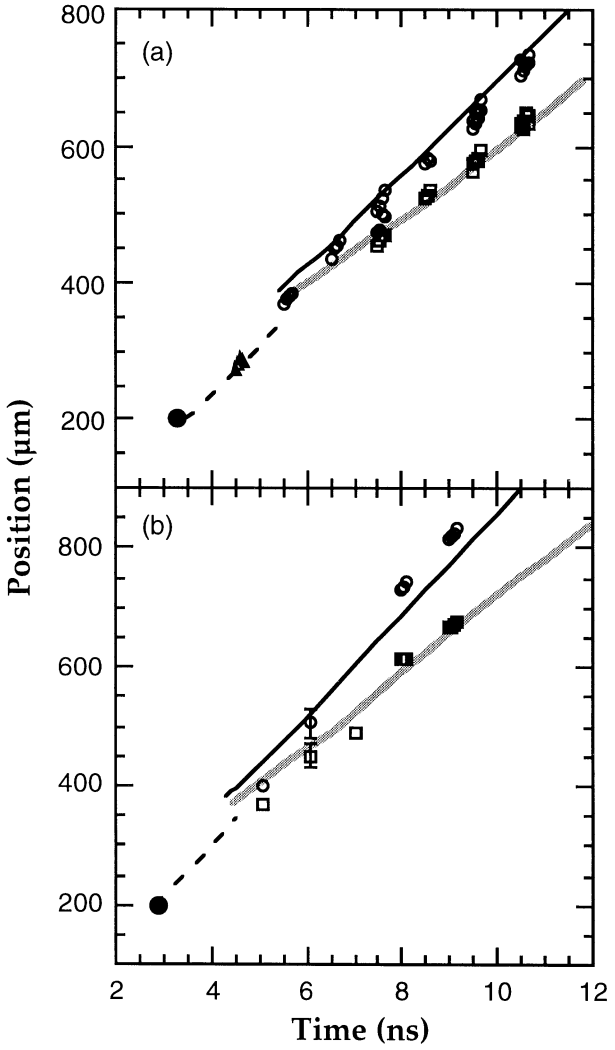

FIG. 4. Data and simulation results for experiments using a plug of (a) $C_{50}H_{44}Br_6$ and (b) $C_{50}H_{48}Br_2$. The uncertainty associated with the data is roughly equal to the symbol size, except in the two cases with error bars. In each case, the observed shock breakout (●), position and time of the forward shock (○), and peak of the stagnated ejecta (□) are shown. In (a), the observed ejecta crossing the gap (△) are also shown, as seen using a 4.3 keV backlighter. The simulation results are as follows: the dashed curve showing the progress of the 0.2 g/cm^3 surface across the gap, the black curve showing the forward shock in the foam, at 0.2 g/cm^3 density, and the gray curve showing the peak of the stagnated ejecta.

astrophysical data. It may also have application to equation of state studies, as a nearly steady shock can be driven for a long time. The stagnated ejecta acts like a classic piston, accelerating and compressing the matter before it.

In conclusion, we have begun the laboratory study of hydrodynamic effects driven by flowing, expanding plasma of high Mach number and high-energy density. We have produced such flowing plasma using an ablative shock as the source and have observed the anticipated forward shock and stagnated ejecta in the system driven by the flow. The quantitative features of one observed system are reproduced well by radiation-hydrodynamic simulations. In another case, there are some differences, which we have discussed. Flow-driven hydrodynamics offers potential as an environment for basic hydrodynamic studies and as a tool for applications from astrophysics to equation of state.

We acknowledge fruitful scientific conversations with A. M. Rubenchik, D. D. Ryutov, Jave Kane, S. Hatchett, A. Benuzzi, J. Dahlburg, and D. Shvarts, scientific contributions to the computations by D. Munro, J. Harte, and G. Zimmerman, tabular EOS data from D. Young, technical support of the experiments by the Nova Facility operations team and the Nova Target Fabrication team, and financial support from the LLNL LDRD-ER Grant No. 97-ERD-022, from the University of Michigan, and support in part under the auspices of the U.S. Department of Energy by the Lawrence Livermore National Laboratory under Contract No. W-7405-ENG-48.

[1] J. D. Lindl, Phys. Plasmas **2**, 3933 (1995).
[2] R. Cauble *et al.*, Phys. Plasmas **4**, 1857 (1997).
[3] B. A. Remington *et al.*, Phys. Plasmas **4**, 1994 (1997).
[4] There is a large literature of such work. Early examples: C. G. M. v.. Kessel and R. Sigel, Phys. Rev. Lett. **33**, 1020 (1974); F. Cottet *et al.*, Phys. Rev. Lett. **52**, 1884 (1984). Recent examples: T. A. Hall *et al.*, Phys. Rev. E **55**, R6356 (1997); D. Hoarty *et al.*, Phys. Rev. Lett. **78**, 3322 (1997).
[5] B. A. Hammel *et al.*, Phys. Fluids B **5**, 2259 (1993).
[6] J. D. Kilkenny *et al.*, Phys. Plasmas **1**, 1379 (1994).
[7] T. Lower *et al.*, Phys. Rev. Lett. **72**, 3186 (1994).
[8] G. Dimonte, C. E. Frerking, and M. Schneider, Phys. Rev. Lett. **74**, 4855 (1995).
[9] M. M. Marinak *et al.*, Phys. Rev. Lett. **75**, 3677 (1995).
[10] T. A. Peyser *et al.*, Phys. Rev. Lett. **75**, 2332 (1995).
[11] B. A. Remington *et al.*, Phys. Plasmas **2**, 241 (1995).
[12] A. Benuzzi *et al.*, Phys. Rev. E **54**, 2162 (1996).
[13] K. S. Budil *et al.*, Phys. Rev. Lett. **76**, 4536 (1996).
[14] W. W. Hsing and N. M. Hoffman, Phys. Rev. Lett. **78**, 3876 (1997).
[15] T. J. Linde *et al.*, J. Geophys. Res. **100**, 1889 (1998).
[16] R. A. Chevalier, Astrophys. J. **258**, 790 (1982).
[17] K. J. Borkowski, J. M. Blondin, and C. L. Sarazin, Astrophys. J **400**, 222 (1992).
[18] R. A. Chevalier, J. M. Blondin, and R. T. Emmering, Astrophys. J. **392**, 118 (1992).
[19] B. I. Jun and M. L. Norman, Astrophys. J. **472**, 245 (1996).
[20] E. M. Campbell *et al.*, Rev. Sci. Instrum. **57**, 2101 (1986).
[21] H. Louis *et al.*, Fusion Tech. **28**, 1833 (1995).
[22] R. L. Kauffman *et al.*, Phys. Rev. Lett. **73**, 2320 (1994).
[23] L. J. Suter *et al.*, Phys. Plasmas **3**, 2057 (1996).
[24] G. B. Zimmerman and W. L. Kruer, Comments Plasma Phys. Controlled Fusion **2**, 51 (1975).
[25] W. A. Lokke and W. Grasberger, Report No. LLNL-UCRL-52276, Nat. Tech. Info. Service, 5285 Port Royal Road, Springfield, VA 22161.
[26] R. M. More *et al.*, Phys. Fluids **31**, 3059 (1988).
[27] G. C. Pomraning, *The Equations of Radiation Hydrodynamics* (Pergamon Press, Oxford, 1973).
[28] K. S. Budil *et al.*, Rev. Sci. Instrum. **67**, 485 (1996).